Journal of Integrative Neuroscience

J. Integr. Neurosci. **2024**; 23(10): 185
https://doi.org/10.31083/j.jin2310185

Original Research

Luteolin Mitigates Dopaminergic Neuron Degeneration and Restrains Microglial M1 Polarization by Inhibiting Toll Like Receptor 4

Yangzhi Xie[1,†], Hao Zhang[1,†], Jiacheng Chen[2], Sicong Xu[1], Yan Luo[1,*]

[1]Department of Neurology, The Affiliated Nanhua Hospital, Hengyang Medical School, University of South China, 421001 Hengyang, Hunan, China
[2]Department of Intensive Care Unit, The Affiliated Nanhua Hospital, Hengyang Medical School, University of South China, 421001 Hengyang, Hunan, China
*Correspondence: luoyan820226@163.com (Yan Luo)
[†]These authors contributed equally.
Academic Editor: Thomas Müller
Submitted: 11 May 2024 Revised: 1 July 2024 Accepted: 12 July 2024 Published: 30 September 2024

Abstract

Background: Luteolin is a natural flavonoid and its neuroprotective and anti-inflammatory effects have been confirmed to mitigate neurodegeneration. Despite these findings, the underlying mechanisms responsible for these effects remain unclear. Toll-like receptor 4 (TLR4) is widely distributed in microglia and plays a pivotal role in neuroinflammation and neurodegeneration. Here studies are outlined that aimed at determining the mechanisms responsible for the anti-inflammatory and neuroprotective actions of luteolin using a rodent model of Parkinson's disease (PD) and specifically focusing on the role of TLR4 in this process. **Methods**: The mouse model of PD used in this experiment was established through a single injection of lipopolysaccharide (LPS). Mice were then subsequently randomly allocated to either the luteolin or vehicle-treated group, then motor performance and dopaminergic neuronal injury were evaluated. BV2 microglial cells were treated with luteolin or vehicle saline prior to LPS challenge. MRNA expression of microglial specific marker ionized calcium-binding adapter molecule 1 (*IBA-1*) and M1/M2 polarization markers, as well as the abundance of indicated pro-inflammatory cytokines in the mesencephalic tissue and BV2 were quantified by real time-polymerase chain reaction (RT-PCR) and Enzyme-linked Immunosorbent Assay (ELISA), respectively. Cell viability and apoptosis of neuron-like PC12 cell line co-cultured with BV2 were detected. TLR4 RNA transcript and protein abundance in mesencephalic tissue and BV2 cells were detected. Nuclear factor kappa-gene binding (NF-κB) p65 subunit phosphorylation both *in vitro* and *in vivo* was evaluated by immunoblotting. **Results**: Luteolin treatment induced functional improvements and alleviated dopaminergic neuronal loss in the PD model. Luteolin inhibited apoptosis and promoted cell survival in PC12 cells. Luteolin treatment shifted microglial M1/M2 polarization towards an anti-inflammatory M2 phenotype both *in vitro and in vivo*. Finally, it was found that luteolin treatment significantly downregulated both *TLR4* mRNA and protein expression as well as restraining NF-κB p65 subunit phosphorylation. **Conclusions**: Luteolin restrained dopaminergic degeneration *in vitro* and *in vivo* by blocking TLR4-mediated neuroinflammation.

Keywords: Parkinson's disease; luteolin; M1/M2 polarization; neuroinflammation; toll like receptor 4

1. Introduction

The clinical features of Parkinson's disease (PD) is rest tremor, rigidity, bradykinesia and disturbance in balance. The pathological alteration of PD is gradually reduction of nigral dopaminergic neurons [1]. The current therapeutic cornerstone of PD is dopamine replacement therapy. However, dopamine replacement therapy is only effective in temporarily attenuating disease symptoms and symptoms eventually worsen. Moreover, extended dopamine use is associated with several side effects [2]. Therefore, emerging PD studies generally focus on phytochemicals for long-term disease symptom modification.

Luteolin is a natural polyphenolic flavonoid compound present in several fruits and vegetables, like chrysanthemum, Perilla species, beets and carrots [3]. The neuroprotective potential of luteolin has been demonstrated in a variety of neurological disorders [4] and previous study has shown that luteolin can reduce neuronal death and cerebral edema in a rodent model of traumatic brain injury [5]. Luteolin also functions in a neuroprotective role in the cognitive dysfunction displayed in an experimental model of epilepsy by inhibiting inflammation and reducing oxidative stress [6]. Depressive-like mice treated with luteolin also show improvement in anxiety behavior [7]. Despite this body of evidence, the exact role and mechanism of luteolin's actions in PD remain unclear.

As the major immune effector cells in the brain. This cell type plays a vital role in central nervous system (CNS) homeostasis, including immune regulation, debris removal and damage repair [8]. Microglia are most dense in the substantia nigra and this specific distribution lays an anatomical foundation for microglia as an important player in PD pathogenesis. Microglia are subdivided into anti-inflammatory M2 and pro-inflammatory M1 phenotypes. Upon stimulation in response to trauma, foreign bodies, infection, microglia are promptly activated into the M1 type

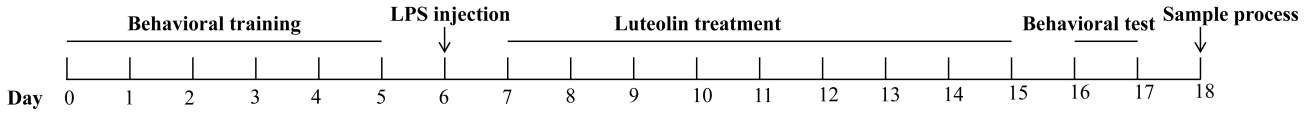

Fig. 1. The schedule used in this study. LPS, lipopolysaccharide.

and its morphology changes with branch protrusions becoming thicker and cell bodies becoming larger [9]. Coordinately, microglia release a large number of inflammatory factors, reactive oxygen species, nitric oxide and superoxide glutamate to both kill pathogenic microorganisms and recruit additional microglia to the lesion site. This activity causes an inflammatory reaction, therefore the M1-type microglia hyperactivation is viewed as a protective reaction for the brain; however, over activation of microglia causes neuronal damage [10].

Activation of microglia may be an initiating factor for Parkinson's disease. Toll-like receptor 4 (TLR4) is ubiquitously distributed in the brain, mostly in microglia and astrocytes. It is the most important pattern recognition receptor expressed in microglia and plays an essential part in inflammatory actions and regulating innate immune [11]. TLR4 recognizes several damage-associated molecular patterns such as heat shock protein 90 (HSP90) and high mobility group box 1 protein (HMGB1) and this both activates microglia and triggers an immune inflammatory cascade [12]. A pre-clinical study has demonstrated that TLR4 activity is related with neuroinflammation and neuronal injury [13]. Clinical data has also confirmed that the abundance of TLR4 in PD patients is significantly elevated and that this effect is closely related to PD progression [14,15].

This study focused on efforts investigating the therapeutic actions of luteolin in both a rodent model of PD and cultured microglial cells. Based on our observations, it is speculated that the anti-inflammatory and neuroprotective actions of luteolin are linked with its ability for limiting TLR4 signaling.

2. Materials and Methods

2.1 Animals and Treatments

All animal experiments were approved by the Affiliated Nanhua Hospital (2024-KY-059). C57BL/6 mice (20–22 g) aged 6–8 weeks were kept with free access to water and food. Mice were trained to adapt a behavioral device for five consecutive days and mice that exhibited poor motor ability in this adjustment were not included in further study. A total of 40 animals were enrolled in this experiment and randomly allocated to each group. On day 6, mice were anesthetized with a mixture of xylazine (7361-61-7; Merck, Rahway, NJ, USA) (10 mg/kg, i.p.) and ketamine (H20023609; Jiuxu Pharmaceutical Co., LTD, Jinhua, Zhejiang, China) (90 mg/kg, i.p.). Following this, mice were injected with lipopolysaccharide (LPS) (5 µg dissolved in 2 µL PBS, C0221A, Beyotime, Shanghai, China) or saline vehicle following stereotaxic coordinates measured from the bregma (Lateral: 1.3 mm; Posterior: 2.8 mm; Ventral to the surface of the dura mater: 4.5 mm). The needle was retained in the left side of the substantia nigra for a period of 10 minutes. The day after LPS injection, mice were intra-peritoneally injected with 40 mg/kg/d luteolin (Catalog: L409168; Aladdin, Shanghai, China), or saline for consecutive 9 days. Subsequently, mice were subjected to behavioral tests to evaluate motor performance on days 16 and 17. Afterward, mice were sacrificed by decapitation, and samples were collected for further analysis. The procedure is given in Fig. 1.

2.2 Cell Cultures and Treatment

BV2 microglia or PC12 neuron-like cells were purchased from Procell Life Science & Technology (Wuhan, Hubei, China) and cultured in Dulbecco's Modified Eagle's Medium (DMEM, Gibco, Anaheim, CA, USA) supplemented with 10% fetal bovine serum (FBS) and 1% streptomycin/penicillin. All cell lines were validated and tested negative for mycoplasma contamination. BV2 and PC12 were both cultured in a 5% CO_2 incubator at 37 °C. BV2 were pretreated with luteolin (40 µM) or saline solution for 3 h after which BV2 were challenged with either LPS (1 µg/mL) or saline (control) for 12 h. For establishing the indirect co-culture system, PC12 was incubated in a 24-well plate for 48 h, BV2 was then transferred to a 0.4 µm pore-sized Transwell insert and co-cultured with PC12 (PC12:BV2 = 2:1) for another 48 h.

2.3 Behavioral Testss

The animals were subjected to rotarod test to examine the strength and coordination. Each mouse was placed on an accelerated rotating rod (30 revolutions per minute) and the latency period to fall from the rod was recorded. If animal did not fall from the rod within 300 seconds, a maximum of 300 seconds was recorded. Each experiment was repeated three times and the mean value was calculated.

A ball wrapped with gauze was fixed on a rough rod (diameter: 0.8 cm; Height: 60 cm). Mice were placed on the ball with its head vertically up. The time it took to completely turn its head downward was recorded as T-turn, and the time it took to climb down to the ground was recorded as T-D. If the mouse fell off the pole, the data was not recorded. When mice stayed on the pole for more than 120 seconds, a maximum value of 120 seconds was recorded.

Table 1. Primers applied for RT-qPCR.

Target gene	Forward primer sequence	Reverse primer sequence
iNOS	GCAGAATGTGACCATCATGG	ACAACCTTGGTGTTGAAGGC
CD32	AATCCTGCCGTTCCTACTGATC	GTGTCACCGTGTCTTCCTTGAG
TNF-α	GTAGCCCACGTCGTAGCAAA	CCCTTCTCCAGCTGGGAGAC
Arg-1	TCACCTGAGCTTTGATGTCG	TTCCCAAGAGTTGGGTTCAC
CD206	AGTTGGGTTCTCCTGTAGCCCAA	ACTACTACCTGAGCCCACACCTGCT
IL-10	CCAAGCCTTATCGGAAATGA	TTTTCACAGGGGAGAAATCG
TLR4	AGTTGATCTACCAAGCCTTGAGT	GCTGGTTGTCCCAAAATCACTTT
IBA-1	CGGGATCCGAGCTATGAGCCAGAGCAAG	GGAATTCCCCACCGTGTTATATCCACC
GAPDH	GTTTGTGATGGGTGTGAACC	TCTTCTGAGTGGCAGTGATG

RT-qPCR, Quantitative Real-time PCR; TLR4, Toll-like receptor 4; iNOS, inducible nitric oxide synthase; TNF-α, tumor necrosis factor-alpha; IBA-1, ionized calcium-binding adapter molecule 1; GAPDH, glyceraldehyde-3-phosphate dehydrogenase; IL, Interleukin; Arg-1, Arginase-1.

2.4 Immunohistochemistry and Immunofluorescence

Animal were transcardially perfused with saline followed by infusion of 4% paraformaldehyde through the left ventricle. Following this, the brain tissue was dissected from the skull, and tissue was placed in 4% paraformaldehyde (PFA) and left overnight at 4 °C, after which the brain tissues were preserved in 30% sucrose solution until the tissue sank. The fixed tissue was sliced using a sliding microtome and brain sections were rinsed and subsequently incubated overnight with primary antibodies (anti-tyrosine hydroxy lase, 1:400; Abcam, Cambridge, UK, cat: ab75875). For immunohistochemistry, sections were incubated with anti-tyrosine hydroxylase (1:400; Abcam, Cambridge, UK, cat: ab75875), followed by enzyme-conjugate IgG (1:50; Beyotime, Shanghai, China) secondary antibodies.

For immunofluorescence, BV2 was incubated with primary antibody against TLR4 (1:100; Santa Cruz, Dallas, TX, USA, cat: sc-293072). After several washings, cells were incubated with goat anti-mouse secondary antibodies CY3 (1:8000; Abcam, Cambridge, UK) in a dark room. The photos were taken using a confocal fluorescence microscope (Leica, Heidelberg, Germany). Immunohistochemistry (IHC) stained cells were examined using a bright-field microscope (Leica, Heidelberg, Germany).

2.5 Liquid Chromatography Tandem Mass Spectrometry (LC-MS/MS)

Appropriate amounts of tissue were exhaustively chopped and homogenized. Following this, tissues were then transferred into a centrifuge tube, and 3 mL of 10% sodium carbonate solution and 10 mL ethyl acetate were added to the tube. Tissues were subsequently homogenized by shaking for 10 min at 4 °C. After centrifugation (6000 r/min for 10 min), the upper layer organic phase was transferred into a pear-shaped bottle and then subjected to rotary evaporation to dry at 40 °C. The residue was dissolved in 1 mL 50% acetonitrile solution and this solution was cooled for 30 min and centrifuged at 16,000 r/min for 5 min. An appropriate amount of the supernatant was filtered through a 0.22 µm membrane and then analyzed by liquid chromatography–mass spectrometry (LC-MS/MS). The devices used in this study are a Waters Acuity UPLC liquid chromatography (Waters, Milford, MA, USA), an AB SCIEX 5500 Qtrap-MS mass spectrography (AB SCIEX, Framingham, MA, USA), and an Acquity UPLC HSS T3 chromatographic column (2.1 µm × 1.8 mm × 100 mm; Waters, USA).

2.6 Quantitative Real-time PCR (RT-qPCR)

Trizol reagent (Sigma-Aldrich, St. Louis, MO, USA) was applied to extract total RNA from BV2 microglial cells or mesencephalic tissue. A PrimeScript RT reagent kit (Takara, Kusatsu, Japan) was then applied to reverse transcribed RNA into cDNA. RT-qPCR was performed using a 7300 Plus Real-time PCR System (Thermo Fisher, Waltham, MA, USA) and an SYBR Green kit (Takara, Japan). Thermocycling was conducted using the following conditions: Denaturation at 95 °C for 15 s, 40 cycles at 95 °C for 10 s, 60 °C for 30 s. Relative quantitative values were calculated using the $2^{-\Delta\Delta Cq}$ method. Each 20 µL reaction mixture contained 10 µL PCR mixture, 1 µL cDNA template, 5 pmol primer, and a proper amount of water. Primers applied in this experiment are outlined in Table 1.

2.7 Enzyme-linked Immunosorbent Assay (ELISA)

The levels of Interleukin (IL)-6, IL-1β, and tumor necrosis factor-alpha (TNF-α) proteins in the mesencephalic tissue and BV2 were determined using Enzyme-linked Immunosorbent Assay (ELISA) following the manufacturer's manual (Beyotime, China).

2.8 Flow Cytometry

PC12 apoptosis when co-cultured with BV2 cells was determined by flow cytometry. PC12 were fixed and permeabilized, cells were subsequently stained with propidium iodide and Annexin (AP101, Multi Sciences, Hangzhou, Zhejiang, China) following the manufacturer's manual.

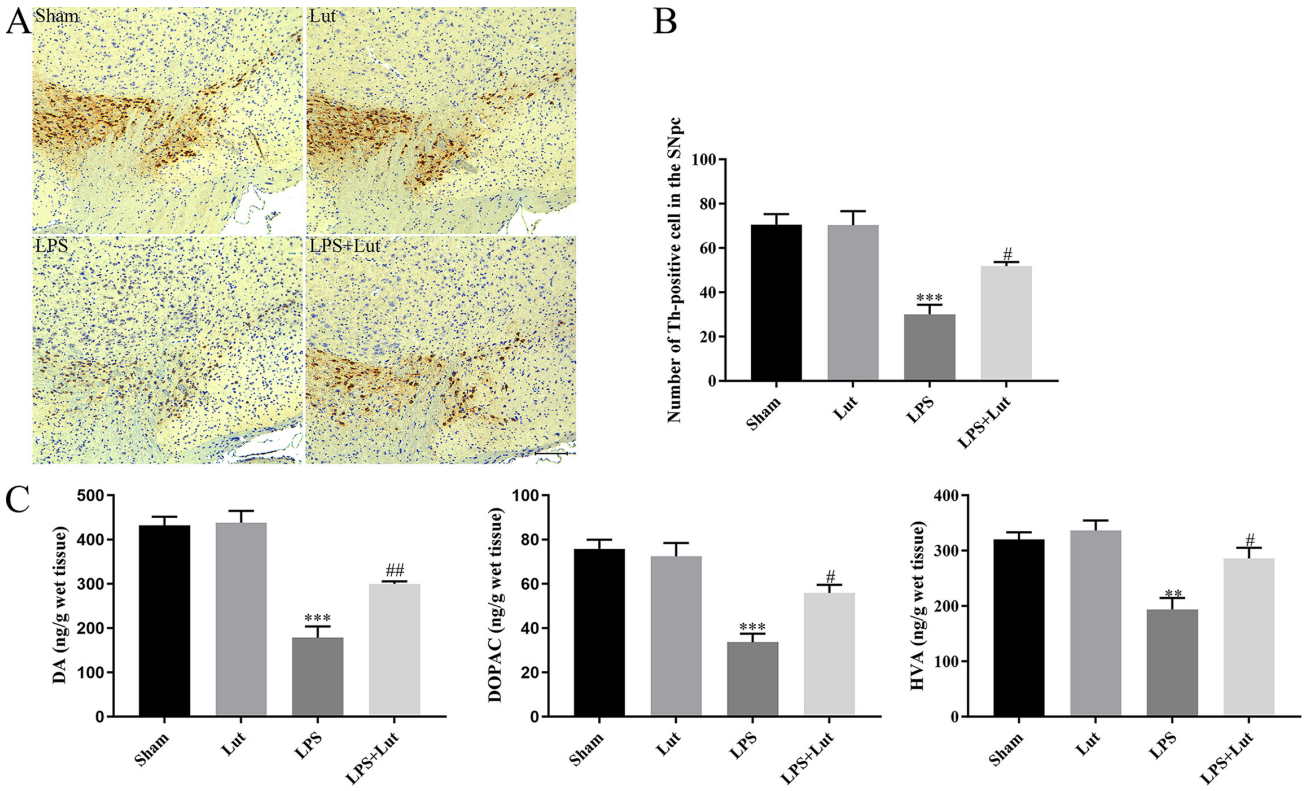

Fig. 2. Luteolin mitigates LPS-induced neuronal injury in the nigrostriatal system of the PD mouse model. (A) Representative immunohistochemical staining for tyrosine hydroxylase in the SN. Scale bar = 100 µm. (B) Th positive cells number within the SN was examined. (C) Abundance of DA, HVA, and DOPAC in the striatum measured by LC-MS/MS. N = 5 per group. $^{**}p < 0.01$, $^{***}p < 0.001$ compared to the sham group. $\#p < 0.05$, $\#\#p < 0.01$ compared to the LPS group. LPS, lipopolysaccharide; PD, Parkinson's disease; DA, dopamine; HVA, homovanillic acid; SN, substantia nigra; DOPAC, dihydroxy-phenyl acetic acid. LC-MS/MS, liquid chromatography–mass spectrometry.

Stained cell preparations were run and analyzed on a flow cytometer (CytoFLEX, Beckman, Pasadena, CA, USA).

2.9 Cell Viability

Cells were seeded into a 96-well plate at 1×10^4 cells per well. A proper amount of Cell Counting kit-8 (CCK-8; Beyotime, C0039, China) buffer was added to each well, and cells were cultured at 37 °C for 2 hours. A microplate reader was used to acquire absorbance at 450 nm.

2.10 Western Blotting

Radio immunoprecipitation assay (RIPA, Beyotime, Shanghai, China) buffer containing Phenylmethanesulfonyl fluoride (PMSF) was applied to homogenize tissues and cells. Proteins were resolved on 10% liquid chromatography-mass spectrometry (SDS-PAGE), and subsequently transferred to the polyvinylidene fluoride (PVDF) membrane. After blocking for 1 hr, membranes were incubated with primary antibody TLR4 (1:100; Santa Cruz, USA, cat: sc-293072), phospho-nuclear factor kappa-gene binding (NF-κB) p65 (1:800; CST, Danvers, MA, USA, cat: #3033), β-actin (1:1000; HuaBio, Hangzhou, Zhejiang, China, cat: ET1701-80), and TATA-binding protein (TBP) (1:1000; HuaBio, China, cat: HA500518). Membranes were subsequently incubated with peroxide-labeled secondary antibodies. Immune complexes were detected using enhanced chemiluminescence (Millipore, Burlington, MA, USA), and results were recorded using a chemiluminescence imaging system (Bio-rad, Berkeley, CA, USA).

2.11 Statistical Analysis

All data presented are expressed as mean $\pm$ SEM. Data were analyzed using one-way ANOVA with Tukey's post-test. Data were analyzed using SPSS 22 software (IBM Corp., Armonk, NY, USA). $p < 0.05$ is considered statistically significant.

3. Results

3.1 Luteolin Treatment Protects against LPS-induced Dopaminergic Neuronal Loss in a PD Animal Model

To assess the neuroprotective responses of luteolin in the outlined PD model, we counted the number of Th positive cells in the substantia nigra (SN) using immunohistochemical staining (Fig. 2A). We found that LPS injection lead to a remarkable decrease of dopaminergic neurons in

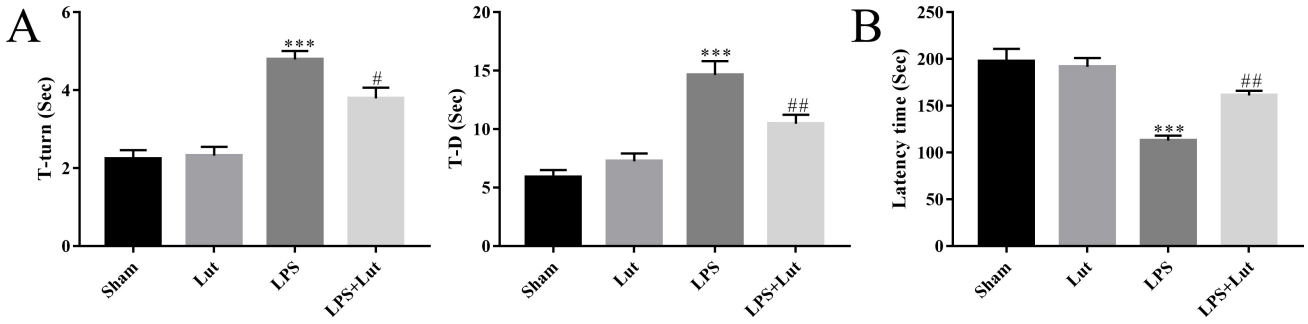

Fig. 3. Luteolin improves motor performance in the PD model. (A) The time for each mouse to turn its head completely downward (T-turn) and climb down to the ground (T-D) was recorded in the pole test. (B) The latency to fall off the rotating rod was recorded in the rotarod test. N = 10 per group. ***$p < 0.001$ compared to the sham group, #$p < 0.05$, ##$p < 0.01$ compared to the LPS group.

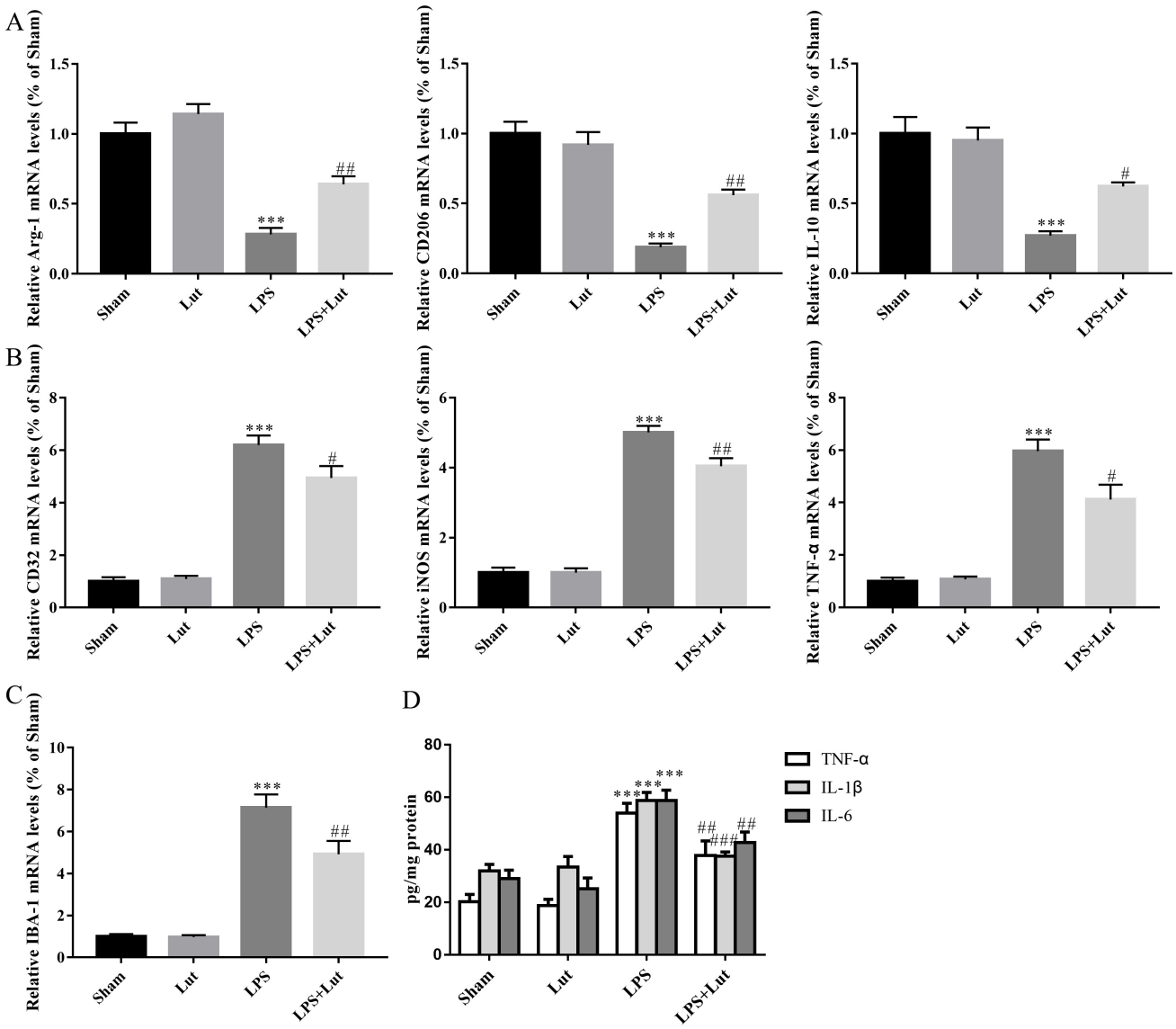

Fig. 4. Luteolin shifts M1/M2 polarization and inhibits the release of pro-inflammatory cytokines in the PD model. (A) Relative mRNA abundance of microglial M2 polarization phenotypic markers *Arg-1*, *CD206*, and *IL-10*. (B) Relative mRNA abundance of microglial M1 polarization markers *CD32*, *iNOS*, and *TNF-α*. (C) Relative mRNA abundance of *IBA-1*. (D) Pro-inflammatory cytokine abundance in the mesencephalic tissue were measured using ELISA. N = 5 per group. ***$p < 0.001$ compared to the sham group; #$p < 0.05$, ##$p < 0.01$, ###$p < 0.001$ compared to the LPS-only group.

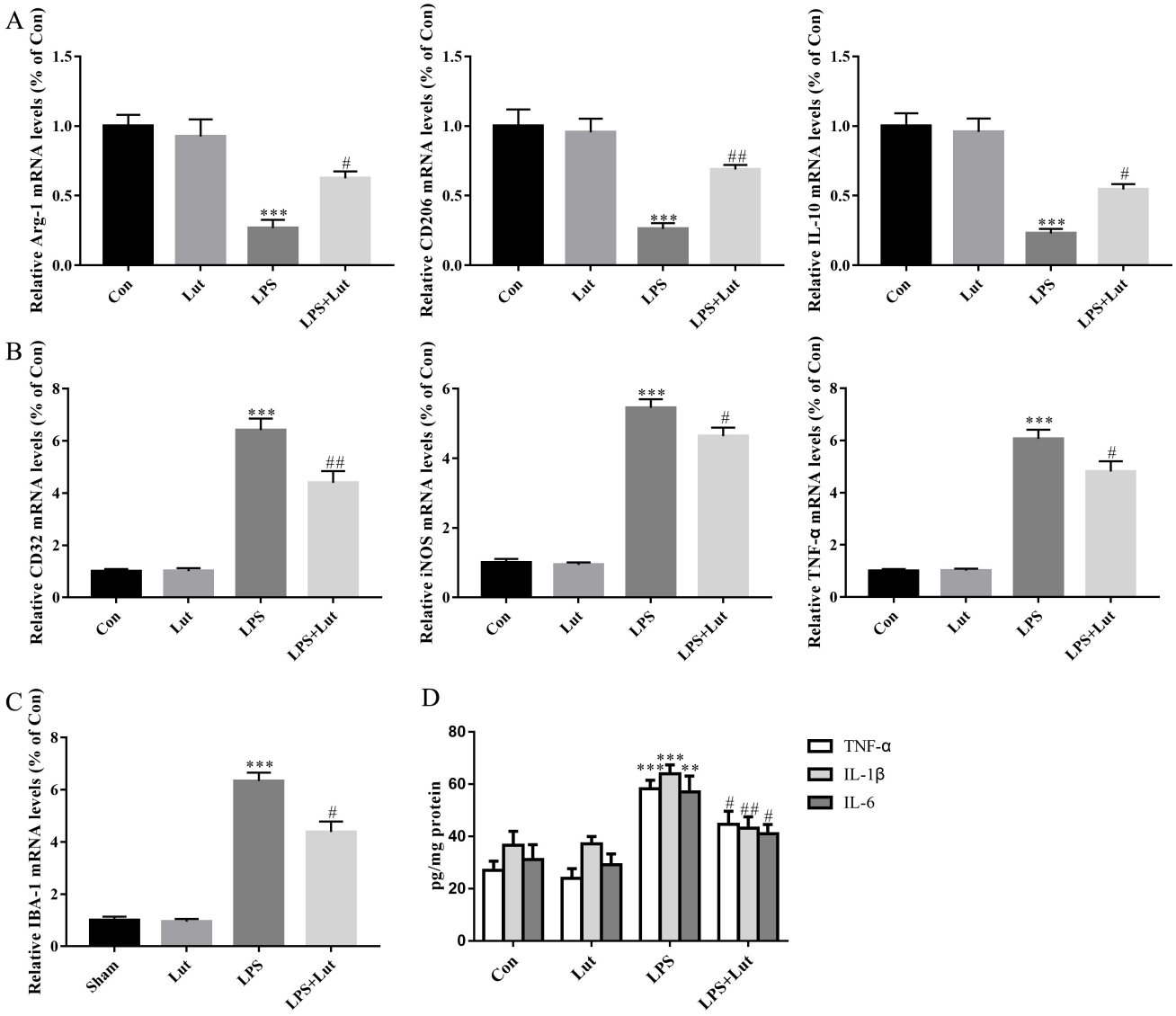

Fig. 5. Luteolin shifts microglial M1/M2 polarization and limited the release of pro-inflammatory cytokines in BV2 microglia cells challenged with LPS. (A) Relative mRNA abundance of microglial M2 phenotypic markers *Arg-1*, *CD206*, and *IL-10*. (B) Relative mRNA abundance of microglial M1 phenotypic markers *CD32*, *iNOS*, and *TNF-α*. (C) Relative mRNA abundance of *IBA-1*. (D) Pro-inflammatory cytokines abundance in BV2 cells were detected using ELISA. N = 5 per group. $^{**}p < 0.01$, $^{***}p < 0.001$ compared to the Control (sham) group, $\#p < 0.05$, $\#\#p < 0.01$ compared to the LPS-only group. ELISA, Enzyme-linked Immunosorbent Assay

the SN ($p < 0.001$, Fig. 2B), and that luteolin treatment attenuated LPS-induced dopaminergic neuronal loss when LPS-only treated mice are compared to the LPS+luteolin group ($p = 0.02$; Fig. 2B). We also measured the abundance of dopamine (DA) and its metabolites, homovanillic acid (HVA) and dihydroxy-phenyl acetic acid (DOPAC) in the striatum using LC-MS/MS. As shown in Fig. 2C, mice injected with LPS lead to decreased abundance of DA ($p < 0.001$), HVA ($p = 0.0016$), and DOPAC ($p < 0.001$) within the striatum. In contrast, treatment with luteolin effectively prevented DA and metabolite loss in the PD model (DA: $p = 0.007$; DOPAC: $p = 0.02$; HVA: $p = 0.016$; Fig. 2C). These data indicated that luteolin alleviates LPS-induced dopaminergic neuronal injury *in vivo*.

3.2 Luteolin Treatment Improves the Motor Ability in the PD Model

Mice were subjected to pole and rotarod tests to assess grip strength and coordination, respectively. LPS injection showed a poorer motor ability in the pole test (T-turn: $p < 0.001$; T-D: $p < 0.001$, Fig. 3A) and rotarod test ($p < 0.001$, Fig. 3B) when compared to sham control animals. Luteolin treatment significantly improved motor performance when compared to LPS-only injected animals in both the pole (T-turn: $p = 0.025$; T-D: $p = 0.007$, Fig. 3A) and rotarod test ($p = 0.003$, Fig. 3B). These data suggest that luteolin treatment can improve motor function in our PD mouse model.

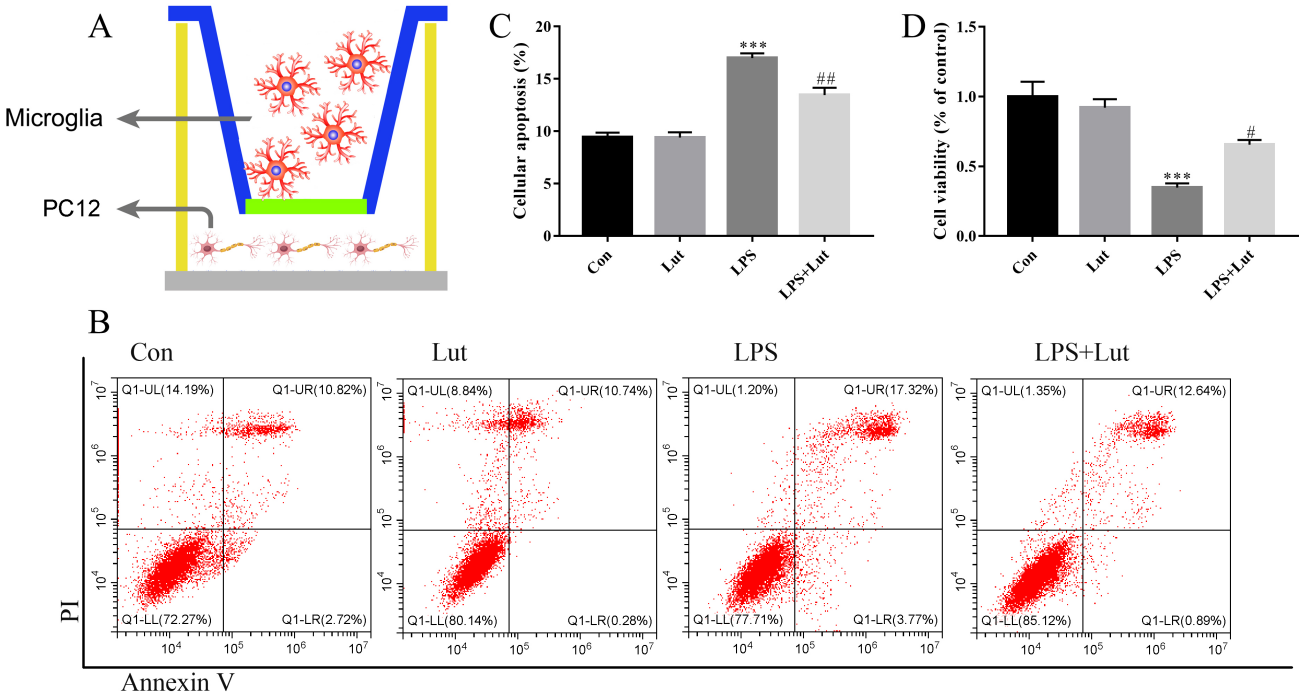

Fig. 6. Luteolin pretreatment before LPS challenging in BV2 rescues neuronal injury in the co-cultured system. (A) A sketch of the co-culture system used. (B) Cellular apoptosis examined by flow cytometry. (C) Bar graph showing the cellular apoptosis. (D) Cell viability was examined by Cell Counting kit-8 (CCK-8). N = 4 per group. ***$p < 0.001$ compared to the control group, #$p < 0.05$, ##$p < 0.01$ compared to the LPS-only group. PI, propidium iodide; UL, up left; UR, up right; LL, low left; LR, low right.

3.3 Luteolin Treatment Shifted M1/M2 Polarization and Restrained the Release of Pro-inflammatory Cytokines in the PD Model

Microglial polarization is vital for neuroinflammation and neuronal degeneration in PD. Thus, we measured relative mRNA abundance of several M1/M2 polarization markers in the midbrain using RT-qPCR. LPS injection reduced anti-inflammatory M2 phenotype markers like Arginase-1 (Arg-1) ($p < 0.001$), CD206 ($p < 0.001$), and IL-10 ($p < 0.001$) when sham control animals were compared to LPS-injected mice (Fig. 4A). In contrast, LPS injection elevated the abundance of pro-inflammatory M1 markers such as CD32 ($p < 0.001$), inducible nitric oxide synthase (iNOS) ($p < 0.001$), and TNF-α ($p < 0.001$) (Fig. 4B). Luteolin treatment significantly increased the level of anti-inflammatory M2 markers Arg-1 ($p = 0.006$), CD206 ($p = 0.005$), IL-10 ($p = 0.029$), when luteolin+LPS mice were compared to LPS-only injected mice (Fig. 4A), and reduced the abundance of M1 markers CD32 ($p = 0.04$), iNOS ($p = 0.006$), and TNF-α ($p = 0.012$) (Fig. 4B). Luteolin treatment in this PD model also restrained microglial hyperactivation, as evidenced by lower ionized calcium-binding adapter molecule 1 (*IBA-1*) mRNA level when compared to LPS-only group ($p = 0.007$, Fig. 4C).

We next measured the abundance of indicated pro-inflammatory cytokines in the midbrain using ELISA. LPS injection resulted in an elevated level of pro-inflammatory cytokine release in the midbrain; specifically, IL-6 ($p < 0.001$), TNF-α ($p < 0.001$), and IL-1β ($p < 0.001$), abundance increased in response to LPS injection (Fig. 4D). This rise in inflammatory cytokines was significantly blunted in response to luteolin treatment (IL-6: $p = 0.009$; TNF-α: $p = 0.009$; IL-1β: $p < 0.001$) when LPS injected mice were compared to those receiving both luteolin and LPS (Fig. 4D). These findings support a potential anti-inflammatory effect for luteolin in this LPS-induced PD mouse model.

3.4 Luteolin Treatment Shifts M1/M2 Polarization and Restrains the Release of Pro-inflammatory Cytokine in BV2 Microglial Cells Challenged with LPS

We next measured relative mRNA levels of M1/M2 phenotypic markers in BV2. As expected, following LPS challenge, BV2 cells exhibited decreased levels of the M2 markers Arg-1 ($p < 0.001$), CD206 ($p < 0.001$), and IL-10 ($p < 0.001$) when compared to the control group (Fig. 5A). Coordinately, we measured increased levels of M1 markers CD32 ($p < 0.001$), iNOS ($p < 0.001$), and TNF-α ($p < 0.001$) following LPS challenge (Fig. 5B). Luteolin pretreatment significantly increased expression of M2 markers Arg-1 ($p = 0.035$), CD206 ($p = 0.009$), and IL-10 ($p = 0.025$) (Fig. 5A), and inhibited the abundance of M1 markers CD32 ($p = 0.002$), iNOS ($p = 0.031$), and TNF-α ($p = 0.02$) compared to mice injected with LPS alone (Fig. 5B). Luteolin pretreatment prior to LPS challenging strikingly limited microglial activation, as evidenced by lower *IBA-1*

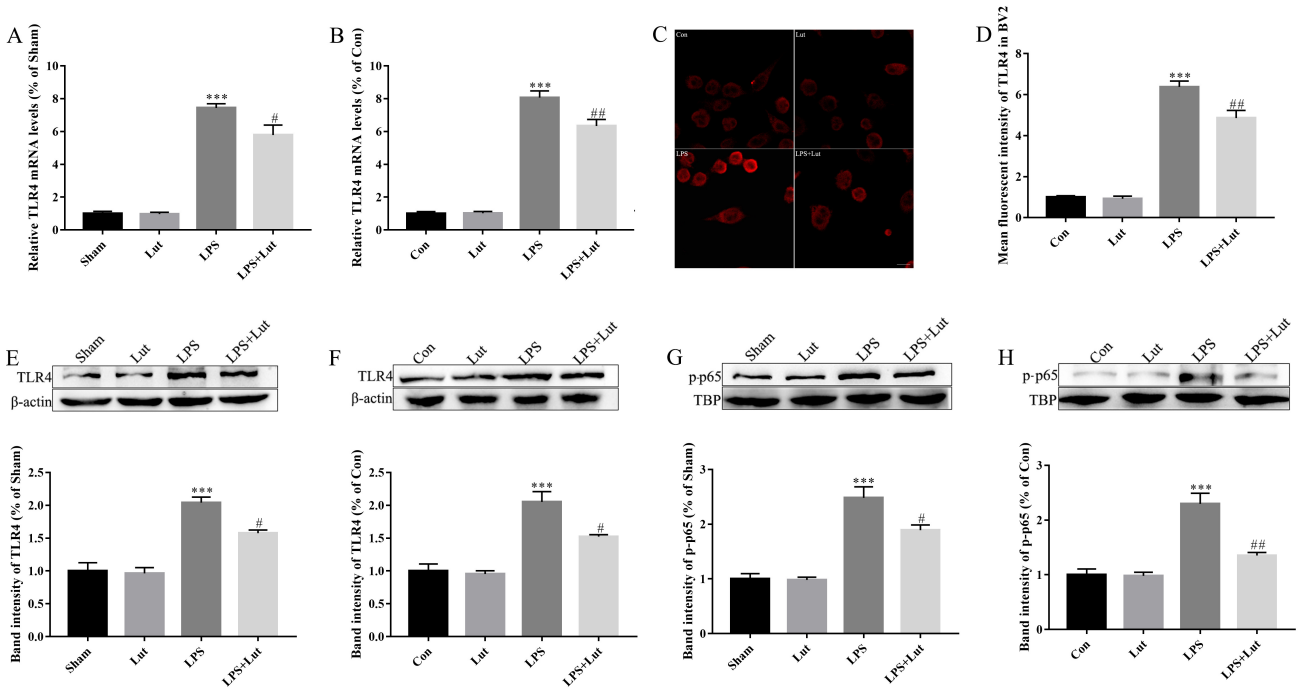

Fig. 7. Luteolin treatment reduces LPS-induced TLR4/NF-κB signaling *in vivo* and *in vitro* model systems. (A) Relative *TLR4* mRNA expression in mesencephalic tissue dissected from mice in the indicated treatment groups. N = 5 measurements per group. (B) Relative *TLR4* mRNA abundance in cultured BV2. N = 5 measurements per group. (C) Representative immunofluorescent confocal images of TLR4 staining in BV2 cells. Scale bar = 20 µm. (D) Mean TLR4 fluorescence intensity in treated and untreated BV2 cells. N = 5 measurements per group. (E) Immunoblots (top) and bar graph of immunoblot quantification (bottom) for TLR4 in mesencephalic tissue. N = 3 per group. (F) Immunoblots (top) and bar graph of immunoblot quantification (bottom) for TLR4 in treated and untreated BV2 cells. N = 3 per group. (G) Immunoblots (top) and bar graph of immunoblot quantification (bottom) for phospho-p65 in mesencephalic tissue. N = 3 per group. (H) Immunoblots (top) and bar graph of immunoblot quantification (bottom) for phospho-p65 in treated and untreated BV2 cells. N = 3 per group. ***$p < 0.001$ compared to the control group, #$p < 0.05$, ##$p < 0.01$ compared to the LPS-only group. NF-κB, nuclear factor kappa-gene binding; TBP, TATA binding protein.

mRNA abundance when compared to LPS-only group (p = 0.027, Fig. 5C). We further observed that luteolin pretreatment reduced LPS-induced pro-inflammatory cytokines release in protein extracts of BV2. Specifically, we measured lower IL-6 (p = 0.038), TNF-α (p = 0.028), and IL-1β (p = 0.003) abundance in BV2 cells following both luteolin and LPS administration (Fig. 5D). These data clearly support an anti-inflammatory effect of luteolin in BV2 cells treated with LPS.

3.5 Luteolin Treatment Rescues LPS-induced Neuronal Injury in a Co-culture System

We established a microglia/neuron indirect co-culture system to explore the neuroprotective actions of luteolin-treated microglia on dopaminergic neurons (Fig. 6A). A 0.4 µm pore-sized membrane was used to separate BV2 and PC12 cells. After treatment with LPS, luteolin, or LPS combined with luteolin, BV2 cells were then transferred to the co-culture system and co-cultured with PC12 for an additional 48 h. After this, PC12 apoptosis was measured by flow cytometry (Fig. 6B), and cell survival was measured using a CCK-8 assay. For the analysis of apoptosis, pretreatment of BV2 cells with luteolin significantly decreased the apoptotic response of PC12 cells (p = 0.002) compared to BV2 cells challenged with LPS-only (Fig. 6C). For the CCK-8 cell viability analysis, pretreatment with luteolin in BV2 prior to LPS administration remarkably increased cell viability of PC12 (p = 0.027) when compared to LPS-only cells (Fig. 6D). These *in vitro* results suggest that luteolin treatment of BV2 cells robustly ameliorates inflammation-induced neuronal injury.

3.6 Luteolin Treatment Reduces LPS-induced Activation of TLR4/NF-κB Pathway in the PD Model and BV2 Cells

TLR4/NF-κB signaling plays a pivotal role in microglial-mediated neuroinflammation. Thus, we next evaluated whether the anti-inflammatory potential of luteolin was associated with TLR4/NF-κB signaling in both *in vivo* and *in vitro* experimental systems. Increased relative *TLR4* mRNA abundance was observed upon LPS challenge in mesencephalic tissue ($p < 0.001$; Fig. 7A) dissected from LPS-treated PD model mice, and in LPS-treated cultured BV2 cells ($p < 0.001$; Fig. 7B). This rise in TLR4 expression was inhibited by luteolin treatment both *in vivo* (p =

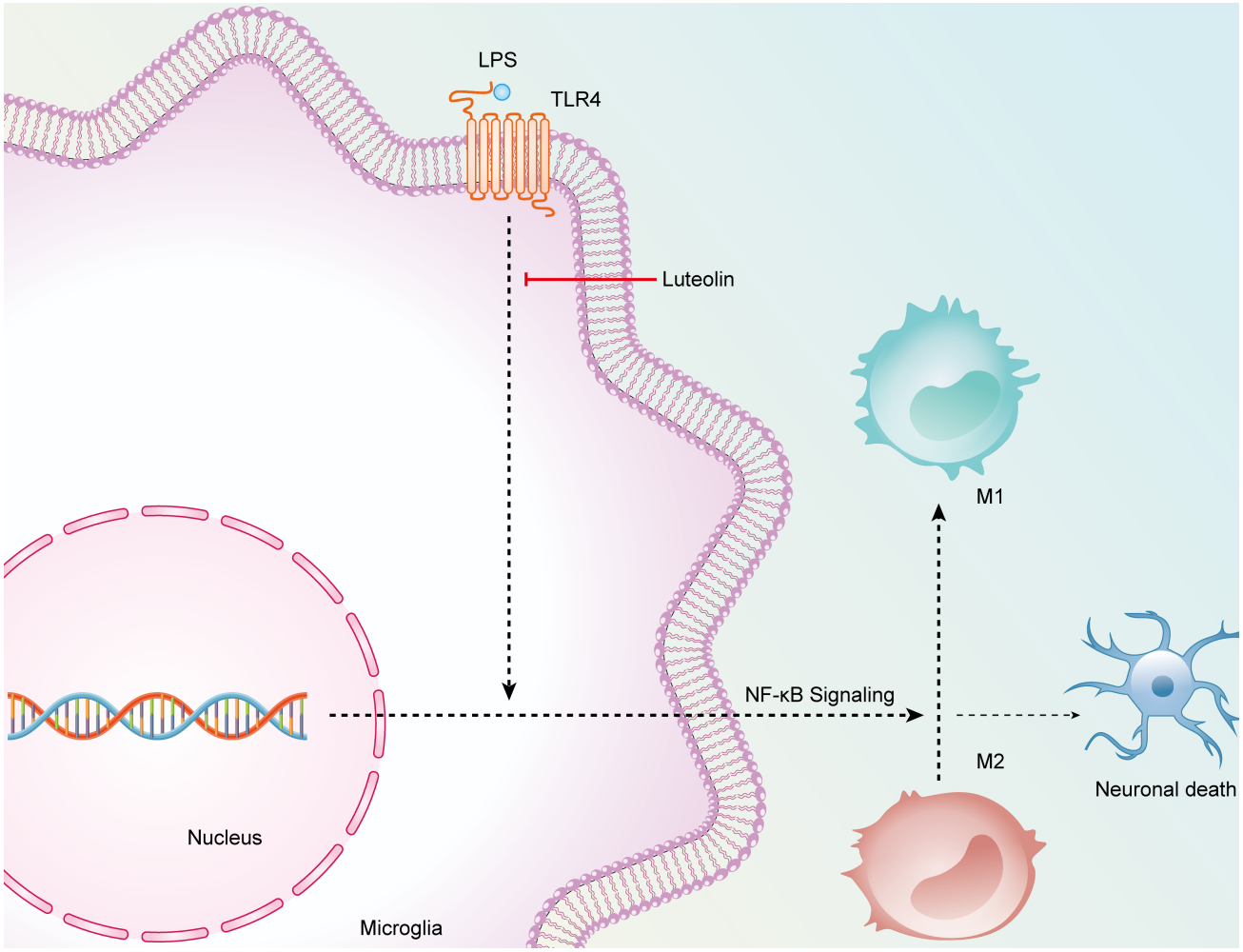

Fig. 8. The schematic diagram elucidating the anti-inflammatory/neuroprotective potential of luteolin.

0.016, Fig. 7A) and *in vitro* ($p = 0.004$; Fig. 7B). We also examined the intensity of TLR4 staining in BV2 cells using immunofluorescence microscopy (Fig. 7C). Compared to the control group, BV2 cells challenged with LPS resulted in a higher intensity of TLR4 staining ($p < 0.001$; Fig. 7D). In contrast, luteolin pretreatment prior to LPS challenge decreased the fluorescence intensity of TLR4 ($p = 0.002$; Fig. 7D). Immunoblot analysis also indicated that luteolin treatment significantly decreased LPS-induced increases in TLR4 within dissected mesencephalic tissue ($p = 0.029$; Fig. 7E) and cultured BV2 cells ($p = 0.016$; Fig. 7F).

LPS treatment was also observed to significantly increase the abundance of phosphorylated (activated) NF-κB subunit p65 both *in vivo* ($p < 0.001$; Fig. 7G) and *in vitro* ($p < 0.001$; Fig. 7H). Luteolin treatment strikingly downregulated LPS-induced, phosphorylated p65 abundance in the PD mouse model ($p = 0.024$; Fig. 7G) and cultured BV2 cells ($p = 0.0035$; Fig. 7H). These data provide evidence that the anti-inflammatory activity of luteolin observed in both the *in vivo* PD model, and *in vitro* cultured microglial cells is likely associated, in part, with diminished TLR4/NF-κB signaling.

4. Discussion

In this study, we explored the neuroprotective actions of luteolin during inflammation-induced dopaminergic injury using both *in vitro* and *in vivo* model systems. The results showed that luteolin treatment induced a functional improvement in this response, and protected against dopaminergic neuronal loss. Luteolin treatment also promoted dopaminergic neuronal survival when PC12 neuronal cells were co-cultured with BV2 microglia challenged with LPS. Moreover, luteolin treatment shifted microglial M1/M2 polarization towards an anti-inflammatory M2 phenotype and blunted pro-inflammatory cytokine release in both *in vitro* and *in vivo* model systems. Mechanistically, our findings suggest that luteolin treatment deactivated TLR4 and downstream NF-κB signaling. The effect of this resulted in an improved inflammatory microenvironment and reduced neuronal loss (Fig. 8).

Microglial polarization imbalance is a key factor in the development of neurodegenerative brain. Moreover, there is the possibility of mutual transformation between M1 and M2 microglial phenotypes corresponding to specific treatments. Therefore, we recognize the potential therapeutic

value in agents that, in situations where phenotypical M1 microglia are over-activated, facilitate the transformation of M1-type microglia into M2 type and maintain a relative balance of M1/M2 cells. Luteolin has a variety of physiological actions *in vivo*, such as anti-inflammatory effects, antioxidant action, and estrogen-like effects [16–18]. In accordance with our findings, a prior study indicates that luteolin functions in a neuroprotective capacity during response to dopaminergic injury by limiting inflammatory response [19]. However, the mechanism(s) that govern such response remain unclear. We found that in LPS-treated PD mouse model and cultured BV2 cells, luteolin intervention restrained the M1-type microglia activation, mitigated the pro-inflammatory cytokines release, and enhanced the activation of anti-inflammatory M2-type microglia resulting in a restoration of the M1/M2 ratio. These effects reduced the neuronal damage that occurs through inflammatory response. In our animal model, we further demonstrated that luteolin significantly blunts both dopaminergic neuronal injury and motor function in inflammation-induced PD mice. Because of limitations stemming from the blood-brain barrier, classic anti-inflammatory drugs are of limited benefit in the treatment of neurological diseases [20]. Luteolin is a highly active natural polyphenol that crosses the blood-brain barrier, thus luteolin is potentially a more robust compound for the treatment and prevention of inflammatory responses mounted within the central nervous system [21].

Although the anti-inflammatory actions of luteolin have been vastly studied, its downstream effector targets remain unclear. Consistent with our results, prior studies have determined that LPS triggers the activation of TLR4 and downstream NF-κB signaling [22,23], thus LPS may generate neuronal degeneration via the canonical TLR4/NF-κB pathway [24,25]. Using TLR4 knock out (KO) mice, prior studies indicate that damage-associated response does not stimulate microglia through the TLR4 pathway [26,27]. This implies that TLR4 deficiency may shape microglia polarization towards the M2 phenotype while inhibiting the M1 phenotype. TLR4 is a type of pattern recognition receptor and once activated, can prompt NF-κB activation through nuclear translocation [28]. Activated NF-κB subsequently promotes the level of pro-inflammatory factors, activates anti-apoptotic genes, and promotes the activation of cell proliferation. Specifically, active NF-κB can promote the expression of IL-6, IL-1β, TNF-α, iNOS, and other inflammatory factors, and regulate microglial polarization [29]. In addition, NF-κB binds to the TLR4 gene promoter and promotes its expression [30]. Thus, harnessing TLR4/NF-κB signaling is a crucial mechanism during the induction of a neuroinflammatory response. In this study, we found that luteolin can decrease TLR4 and p65 phosphorylation, indicating that TLR4/NF-κB pathway is, at least in part, a target for luteolin in limiting neuroinflammation and dopaminergic neuron degeneration.

We note some limitations in this study. For example, the concentration of luteolin in mouse brain tissue is unclear. More reliable methods for judging drug distribution are needed to better understand how luteolin reaches the brain. Tissue distribution of luteolin may be considered using *in vivo* imaging of animals or through high performance liquid chromatography (HPLC) approaches. In addition, the anti-inflammatory effect of luteolin in TLR4-overexpressing microglial cells requires further examination.

5. Conclusions

In summary, our results indicate that luteolin protects against inflammation-induced dopaminergic neuronal loss. Mechanistically, luteolin deactivated TLR4/NF-κB signaling in microglia, shifting microglial polarization towards anti-inflammatory M2 phenotupe, thus improving the inflammatory niche and subsequently attenuating dopaminergic neuronal loss both *in vitro* and *in vivo*. Luteolin has limited adverse reactions and displays low toxicity, and thus has broad application prospects as a PD therapeutic.

Availability of Data and Materials

The data used and analyzed during the current study are available on reasonable request.

Author Contributions

YX, HZ, JC, SX and YL performed the research. YX, HZ, and SX analyzed the data. All authors contributed to editorial changes in the manuscript. All authors read and approved the final manuscript. All authors have participated sufficiently in the work and agreed to be accountable for all aspects of the work.

Ethics Approval and Consent to Participate

The animal study protocol was approved by the Institutional Review Board of The Affiliated Nanhua Hospital (protocol code: 2024-KY-059).

Acknowledgment

We thank Ejear Editing for the preparation of the manuscript.

Funding

This work was supported by Natural Science Foudation Of Hunan Province (grant number 2023JJ50159).

Conflict of Interest

The authors declare no conflict of interest.

References

[1] Tolosa E, Garrido A, Scholz SW, Poewe W. Challenges in the diagnosis of Parkinson's disease. The Lancet. Neurology. 2021; 20: 385–397.

[2] Elkouzi A, Vedam-Mai V, Eisinger RS, Okun MS. Emerging therapies in Parkinson disease - repurposed drugs and new approaches. Nature Reviews. Neurology. 2019; 15: 204–223.
[3] Cordaro M, Cuzzocrea S, Crupi R. An Update of Palmitoylethanolamide and Luteolin Effects in Preclinical and Clinical Studies of Neuroinflammatory Events. Antioxidants (Basel, Switzerland). 2020; 9: 216.
[4] Calis Z, Mogulkoc R, Baltaci AK. The Roles of Flavonols/Flavonoids in Neurodegeneration and Neuroinflammation. Mini Reviews in Medicinal Chemistry. 2020; 20: 1475–1488.
[5] Xu J, Wang H, Lu X, Ding K, Zhang L, He J, *et al*. Posttraumatic administration of luteolin protects mice from traumatic brain injury: implication of autophagy and inflammation. Brain Research. 2014; 1582: 237–246.
[6] Zhen JL, Chang YN, Qu ZZ, Fu T, Liu JQ, Wang WP. Luteolin rescues pentylenetetrazole-induced cognitive impairment in epileptic rats by reducing oxidative stress and activating PKA/CREB/BDNF signaling. Epilepsy & Behavior: E&B. 2016; 57: 177–184.
[7] Achour M, Ferdousi F, Sasaki K, Isoda H. Luteolin Modulates Neural Stem Cells Fate Determination: *In vitro* Study on Human Neural Stem Cells, and *in vivo* Study on LPS-Induced Depression Mice Model. Frontiers in Cell and Developmental Biology. 2021; 9: 753279.
[8] Borst K, Dumas AA, Prinz M. Microglia: Immune and non-immune functions. Immunity. 2021; 54: 2194–2208.
[9] Savage JC, Carrier M, Tremblay MÈ. Morphology of Microglia Across Contexts of Health and Disease. Methods in Molecular Biology (Clifton, N.J.). 2019; 2034: 13–26.
[10] Guo S, Wang H, Yin Y. Microglia Polarization From M1 to M2 in Neurodegenerative Diseases. Frontiers in Aging Neuroscience. 2022; 14: 815347.
[11] Heidari A, Yazdanpanah N, Rezaei N. The role of Toll-like receptors and neuroinflammation in Parkinson's disease. Journal of Neuroinflammation. 2022; 19: 135.
[12] Pan PH, Wang YY, Lin SY, Liao SL, Chen YF, Huang WC, *et al*. Plumbagin ameliorates bile duct ligation-induced cholestatic liver injury in rats. Biomedicine & Pharmacotherapy = Biomedecine & Pharmacotherapie. 2022; 151: 113133.
[13] Azam S, Jakaria M, Kim IS, Kim J, Haque ME, Choi DK. Regulation of Toll-Like Receptor (TLR) Signaling Pathway by Polyphenols in the Treatment of Age-Linked Neurodegenerative Diseases: Focus on TLR4 Signaling. Frontiers in Immunology. 2019; 10: 1000.
[14] Kouli A, Horne CB, Williams-Gray CH. Toll-like receptors and their therapeutic potential in Parkinson's disease and α-synucleinopathies. Brain, Behavior, and Immunity. 2019; 81: 41–51.
[15] Yang Y, Han C, Guo L, Guan Q. High expression of the HMGB1-TLR4 axis and its downstream signaling factors in patients with Parkinson's disease and the relationship of pathological staging. Brain and Behavior. 2018; 8: e00948.
[16] Wang S, Cao M, Xu S, Shi J, Mao X, Yao X, *et al*. Luteolin Alters Macrophage Polarization to Inhibit Inflammation. Inflammation. 2020; 43: 95–108.
[17] Li L, Luo W, Qian Y, Zhu W, Qian J, Li J, *et al*. Luteolin protects against diabetic cardiomyopathy by inhibiting NF-κB-mediated inflammation and activating the Nrf2-mediated antioxidant responses. Phytomedicine: International Journal of Phytotherapy and Phytopharmacology. 2019; 59: 152774.
[18] Wang X, Zhang L, Dai Q, Si H, Zhang L, Eltom SE, *et al*. Combined Luteolin and Indole-3-Carbinol Synergistically Constrains ERα-Positive Breast Cancer by Dual Inhibiting Estrogen Receptor Alpha and Cyclin-Dependent Kinase 4/6 Pathway in Cultured Cells and Xenograft Mice. Cancers. 2021; 13: 2116.
[19] Qin L, Chen Z, Yang L, Shi H, Wu H, Zhang B, *et al*. Luteolin-7-O-glucoside protects dopaminergic neurons by activating estrogen-receptor-mediated signaling pathway in MPTP-induced mice. Toxicology. 2019; 426: 152256.
[20] Ronaldson PT, Davis TP. Regulation of blood-brain barrier integrity by microglia in health and disease: A therapeutic opportunity. Journal of Cerebral Blood Flow and Metabolism: Official Journal of the International Society of Cerebral Blood Flow and Metabolism. 2020; 40: S6–S24.
[21] Shimazu R, Anada M, Miyaguchi A, Nomi Y, Matsumoto H. Evaluation of Blood-Brain Barrier Permeability of Polyphenols, Anthocyanins, and Their Metabolites. Journal of Agricultural and Food Chemistry. 2021; 69: 11676–11686.
[22] Ryu JK, Kim SJ, Rah SH, Kang JI, Jung HE, Lee D, *et al*. Reconstruction of LPS Transfer Cascade Reveals Structural Determinants within LBP, CD14, and TLR4-MD2 for Efficient LPS Recognition and Transfer. Immunity. 2017; 46: 38–50.
[23] Lai JL, Liu YH, Liu C, Qi MP, Liu RN, Zhu XF, *et al*. Indirubin Inhibits LPS-Induced Inflammation via TLR4 Abrogation Mediated by the NF-κB and MAPK Signaling Pathways. Inflammation. 2017; 40: 1–12.
[24] Ahmad A, Ali T, Rehman SU, Kim MO. Phytomedicine-Based Potent Antioxidant, Fisetin Protects CNS-Insult LPS-Induced Oxidative Stress-Mediated Neurodegeneration and Memory Impairment. Journal of Clinical Medicine. 2019; 8: 850.
[25] Zhang FX, Xu RS. Juglanin ameliorates LPS-induced neuroinflammation in animal models of Parkinson's disease and cell culture via inactivating TLR4/NF-κB pathway. Biomedicine & Pharmacotherapy. 2018; 97: 1011–1019.
[26] Wang H, Huang M, Wang W, Zhang Y, Ma X, Luo L, *et al*. Microglial TLR4-induced TAK1 phosphorylation and NLRP3 activation mediates neuroinflammation and contributes to chronic morphine-induced antinociceptive tolerance. Pharmacological Research. 2021; 165: 105482.
[27] Nie X, Kitaoka S, Tanaka K, Segi-Nishida E, Imoto Y, Ogawa A, *et al*. The Innate Immune Receptors TLR2/4 Mediate Repeated Social Defeat Stress-Induced Social Avoidance through Prefrontal Microglial Activation. Neuron. 2018; 99: 464–479.e7.
[28] Gurram PC, Manandhar S, Satarker S, Mudgal J, Arora D, Nampoothiri M. Dopaminergic Signaling as a Plausible Modulator of Astrocytic Toll-Like Receptor 4: A Crosstalk between Neuroinflammation and Cognition. CNS & Neurological Disorders Drug Targets. 2023; 22: 539–557.
[29] Sun E, Motolani A, Campos L, Lu T. The Pivotal Role of NF-κB in the Pathogenesis and Therapeutics of Alzheimer's Disease. International Journal of Molecular Sciences. 2022; 23: 8972.
[30] Troutman TD, Kofman E, Glass CK. Exploiting dynamic enhancer landscapes to decode macrophage and microglia phenotypes in health and disease. Molecular Cell. 2021; 81: 3888–3903.